Journal of Power Sources 196 (2011) 7182–7187

Contents lists available at ScienceDirect

Journal of Power Sources

journal homepage: www.elsevier.com/locate/jpowsour

The effect of current density on H_2S-poisoning of nickel-based solid oxide fuel cell anodes

E. Brightman[a,*], D.G. Ivey[b], D.J.L. Brett[c], N.P. Brandon[a]

[a] Department of Earth Science and Engineering, Imperial College London, London SW7 2AZ, UK
[b] Department of Chemical and Materials Engineering, University of Alberta, Edmonton, Alberta, Canada T6G 2V4
[c] Department of Chemical Engineering, University College London, Torrington Place, London WC1E 7JE, UK

ARTICLE INFO

Article history:
Received 30 June 2010
Received in revised form
24 September 2010
Accepted 29 September 2010
Available online 7 October 2010

Keywords:
Solid oxide fuel cell
Sulphur poisoning
Ceria
Ni–GDC
Electrochemistry
Impedance spectroscopy

ABSTRACT

Sulphur-containing impurities can have a damaging impact on nickel-based SOFC anode performance even at sub-ppm concentrations, but the electrochemical mechanism of this interaction is not fully understood. In this work, three-electrode cells of Ni-$Ce_{0.9}Gd_{0.1}O_{1.95}$/YSZ/$(La_{0.8}Sr_{0.2})MnO_{3-x}$ have been used to obtain new electrochemical data on the sulphur poisoning behaviour of Ni-based SOFC anodes operating at different current densities in the temperature range 700–750 °C. The three-electrode arrangement enabled direct measurement of anode overpotential, with concurrent impedance measurement to provide detail into the electrochemical processes occurring at the anode during sulphur poisoning.

The initial, stepwise degradation on exposure to 0.5 ppm H_2S caused an increase in anode polarization resistance, which was almost entirely recoverable on removal of H_2S. Operation at higher current density was found to result in a smaller increase in anode polarization resistance. It is proposed that this initial poisoning behaviour is caused by adsorbed sulphur inhibiting surface diffusion of H atoms to active sites.

Exposure to 1 ppm and 3 ppm levels of H_2S led to an observed secondary degradation which was also recoverable on removal of sulphur. This degradation was caused by an increased ohmic resistance, and was more severe at higher temperatures. The authors discuss possible explanations for this behaviour.

1. Introduction

Sulphur-containing impurities are present in most fuels suitable for solid oxide fuel cells (SOFC). Sulphur is known to be a poison to nickel and other catalysts [1–8], but it is expensive to remove completely, and the effects of sulphur on SOFC anodes are not yet fully understood. There have been many previous studies, mostly on Ni–YSZ anodes with H_2/H_2S fuel mixtures, across a wide range of H_2S concentrations (0.05 ppm to several thousand ppm) and temperatures (600–1000 °C) [3,8,9]. The most important trends to draw from these studies are that the extent of sulphur poisoning increases with sulphur concentration, and decreases at a given concentration with increasing temperature. The most interesting and relevant conditions applicable to state-of-the-art SOFCs with partially desulphurized fuel are for pH_2S around 0.1–10 ppm and temperatures between 700 and 800 °C. These conditions may be applicable for a commercial SOFC operating on natural gas that has been passed through a simple desulphurizer unit, or where breakthrough of sulphur impurity arises from desulphurizer failure.

Several researchers have used d.c. polarization techniques to show that within the above operating range there is an initial reversible (or partially reversible) degradation step over a number of minutes when H_2S is first introduced, followed by a much slower irreversible degradation over several hours [3,10]. Impedance spectroscopy has also been used to show that the drop in cell power output is attributable to an increase in anode polarization resistance [3,11]. This is consistent with a mechanism involving adsorption of S on the Ni surface causing blockage of active sites for H adsorption and oxidation.

Cheng et al. [12] have shown that the increase in anode polarization resistance, rather than the drop in cell power output, should be used to describe the extent of sulphur poisoning when investigating the influence of cell voltage or current. If the drop in power output is used, then there is an apparent contradiction in the effect of potential or current density on the extent of poisoning, depending on whether the cell is operated under galvanostatic or potentiostatic control.

For longer-term (several hours or more) exposure to a sulphur-containing fuel, a slow irreversible increase in ohmic resistance is sometimes observed [3,8]. This has been suggested to arise from bulk nickel sulphide formation, such as Ni_3S_2, which would cause a drop in conductivity of the anode. However, thermodynamic calculations have shown that under usual SOFC operating condi-

* Corresponding author. Tel.: +44 207 594 9980; fax: +44 207 594 7444.
E-mail address: e.brightman07@imperial.ac.uk (E. Brightman).

0378-7753/$ – see front matter © 2010 Elsevier B.V. All rights reserved.
doi:10.1016/j.jpowsour.2010.09.089

tions, i.e., $pH_2S < 100$ ppm at $T > 600\,^{\circ}C$, Ni_3S_2 would spontaneously decompose to Ni and H_2S [13]. The authors have recently reported observations of surface reconstruction of Ni grains induced by S adsorption [14], causing step formation, which may be indicative of S dissolution in the surface of Ni.

Nickel/gadolinium-doped ceria (Ni-CGO) anodes are of interest for use in intermediate-temperature SOFCs, which have many advantages in terms of manufacturing and operating costs [15]. The effects of sulphur impurities are much more important as temperature is lowered, however, because S adsorbs more strongly on Ni at lower temperatures.

In this work, three-electrode measurements of SOFCs at 700–750 °C using combined electrochemical impedance spectroscopy (EIS) and d.c. potentiometry have been performed to investigate the effect of current density on the increase in anode polarization resistance due to sulphur poisoning for Ni–CGO anodes. Higher current densities were found to give rise to a lower increase in polarization resistance in the presence of sulphur, as well as a faster recovery on the removal of sulphur. The operating temperature and sulphur concentration were also varied and a secondary degradation mechanism was observed over a period of 2–3 h. This is thought to be a result of dissolution of sulphur in the nickel surface forming a barrier to electronic conduction.

2. Experimental

Electrolyte supported button cells in a three-electrode configuration were fabricated with nickel–gadolinium-doped ceria (Ni–CGO) anodes, yttria-stabilised zirconia (YSZ) electrolytes, and lanthanum-strontium-manganate (LSM–YSZ) cathodes and reference electrodes. 8 mol% YSZ electrolyte powder (TZ-8Y, Tosoh, Japan) was uniaxially die-pressed and sintered at 1450 °C for 5 h to give dense pellets 1.25 mm ± 0.05 mm thick and 23 mm diameter. Cermet anodes of 60 wt% NiO:40 wt% $Ce_{0.9}Gd_{0.1}O_{1.95}$ (Fuel Cell Materials, USA) were screen printed and sintered at 1350 °C for 1 h. Cathodes and reference electrodes of 50 wt% $(La_{0.8}Sr_{0.2})MnO_{3-x}$:50 wt% $(Y_2O_3)_{0.08}(ZrO_2)_{0.92}$ (Fuel Cell Materials, USA) were then screen printed and sintered at 1150 °C for 1 h. The electrode geometry used for the anode was a circular disc 11 mm in diameter with a surface area of 0.95 cm^2 and the cathode was an identical circular disc, surrounded by a ring with an internal diameter of 17 mm, and an external diameter of 19 mm. The thickness of the electrodes was in the range 30–70 μm.

The cell was attached to the end of an alumina tube using Ceramabond™ 503 alumina-based ceramic paste (Aremco, USA), with fuel gas supplied through a narrower alumina tube directly to the anode inside the larger tube. The cathode was open to stagnant ambient laboratory air such that oxygen depletion was negligible for the duration of the experiment. Platinum mesh was used for electrical contact, with gold paste on the counter and reference electrodes to improve the surface conductivity, and external tension-springs for contact pressure. The cell temperature was monitored with a type K thermocouple positioned ~5 mm above the surface of the counter electrode. Hydrogen and nitrogen gases were passed through a water bubbler in a temperature-controlled water bath to achieve humidification to ~2% H_2O. The anode was reduced at 800 °C by increasing the H_2 concentration stepwise as follows: 4.9% (30 min), 9.8% (15 min), 14.7% (15 min) and 24.5% (30 min). The furnace was then ramped down to the operating temperature at a rate of 7.5 °C min^{-1}, and the gas composition was changed to 49% H_2, 49% N_2 and 2% H_2O. For the sulphur poisoning experiments the hydrogen was diverted to bypass the water bubbler and the water bath was heated to 35 °C to achieve 4% H_2O in the nitrogen, which, when mixed 50:50 with the fuel gas, gave the desired 2% H_2O. The pure hydrogen was mixed in various proportions with hydrogen containing 10 ppm H_2S, to achieve H_2S concentrations of 0.5, 1, and 3 ppm in 50% H_2, 2%H_2O, and 48% N_2 at a total flow rate of 100 cm^3 min^{-1}.

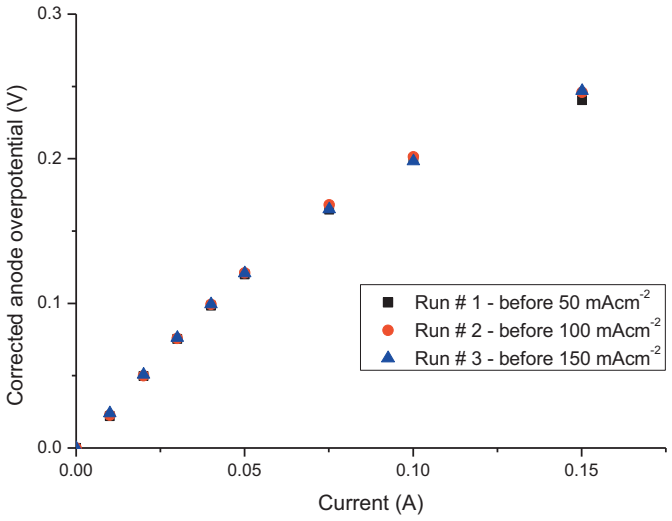

Fig. 1. Polarization performance of test cell for Section 3.1 before each successive H_2S exposure. $T = 715\,^{\circ}C$, 49% H_2, 49% N_2, 2% H_2O.

Electrochemical impedance measurements and potentiometry were carried out under galvanostatic control using an Autolab PGSTAT302 (Eco Chemie, The Netherlands) with an FRA module. Autolab Nova software v1.5 was used for control and analysis of the measurements.

Cells were first characterized in clean fuel using the overpotential correction procedure described in Offer et al. [16], which involves using EIS to compensate for errors in the measured overpotential due to non-ideal reference electrode geometry. The cells were then held galvanostatically at the specified current density for the poisoning and recovery test. The cell potential was measured every 10 s and impedance was measured every 25 min with an amplitude of 10 mA (r.m.s.) across the frequency range 9.9 kHz to 0.05 Hz for the sulphur poisoning experiments.

3. Results and analysis

3.1. Effect of current density

A cell operated at 715 °C was exposed to 0.5 ppm H_2S in 49% H_2/49% N_2/2% H_2O as described above and recovered in clean fuel successively at three different current densities. The cell was characterized by an i-V measurement with impedance compensation as described in Ref. [16] between each successive poisoning (Fig. 1). The measured performance was consistent with a background degradation rate of <1% over the duration of the test.

An example of the typical impedance spectra measured during the degradation test is shown in Fig. 2(A). The spectra were fitted to an equivalent circuit shown in Fig. 2(B) consisting of a series resistance R_s and two *R-CPE* parallel elements (*CPE* = constant phase element), using Z-View v3.0 (Scribner Associates, USA). It was found that only the low frequency semicircle ($\nu_{max} \approx 1$ Hz) was affected by the presence of sulphur, referred to here as R_p (*LF*), which is consistent with other studies [3,12]. The frequency range of this arc is consistent with the range expected for diffusion-related processes [17].

Current densities of 0.05 A cm^{-2}, 0.10 A cm^{-2} and 0.15 A cm^{-2} were used. The measured cell potential E was converted to give an uncompensated anode resistance between working electrode and reference electrode (here given as the symbol $R_{WE\text{-}RE}$) by the

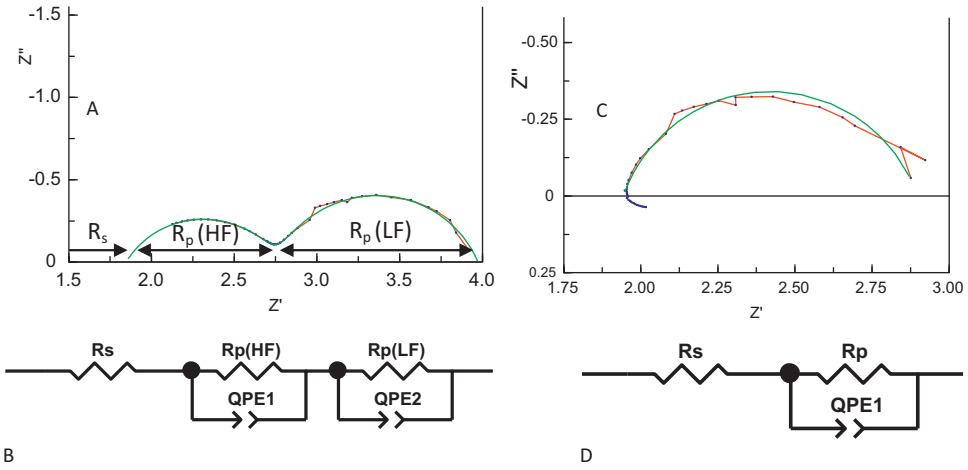

Fig. 2. Examples of impedance spectra taken at regular intervals during the potentiometry experiments, and equivalent circuits used for fitting, in (A) and (B) Section 3.1 and (C) and (D) Section 3.2.

formula $R_{WE\text{-}RE} = (E - E_0)/i$ where E_0 is the measured OCP and i is the current density. Uncompensated anode resistance is plotted in Fig. 3 along with the R_s and R_p (LF) values extracted from the periodic impedance measurements by an equivalent circuit model, as described above. The R_s value is attributed to the component of impedance from the electrolyte between the reference electrode and the working electrode, with some contribution from the current collector leads. By assuming these values remain unchanged during the potentiometry measurement, it is possible to subtract R_s from $R_{WE\text{-}RE}$ to obtain a measurement of the anode interfacial resistance, as plotted in Fig. 4.

There is a continuous linear increase in the R_s component with time observable in Fig. 3(B), which shows that the series resistance of the cell was slightly higher for each successive run (measurements were performed in the order 0.05 A cm^{-2}, 0.10 A cm^{-2}, 0.15 A cm^{-2}, on consecutive days). This trend is clearly due to background degradation in the cell. However, the anode polarization resistance shown in Figs. 3(C) and 4 is significantly lower overall as current density increases. This is a result of lower charge-transfer resistance and is consistent with the i-V behaviour of the cell shown in Fig. 1.

Fig. 5 shows the difference in anode resistance in the presence of H_2S and in clean fuel at the three different current densities studied, as measured from both the continuous potentiometry data and the impedance data. The correlation between the two quantities suggests that the increase in cell resistance observed on sulphur poisoning arises entirely from the anode low-frequency impedance.

The degree of poisoning is lower for higher current density, which is consistent with the results obtained by Cheng et al. for a Ni–YSZ anode [12], and suggests that adsorbed sulphur atoms are oxidized electrochemically at the triple-phase boundary as in Eq. (1), since a higher current density means there is a higher flux

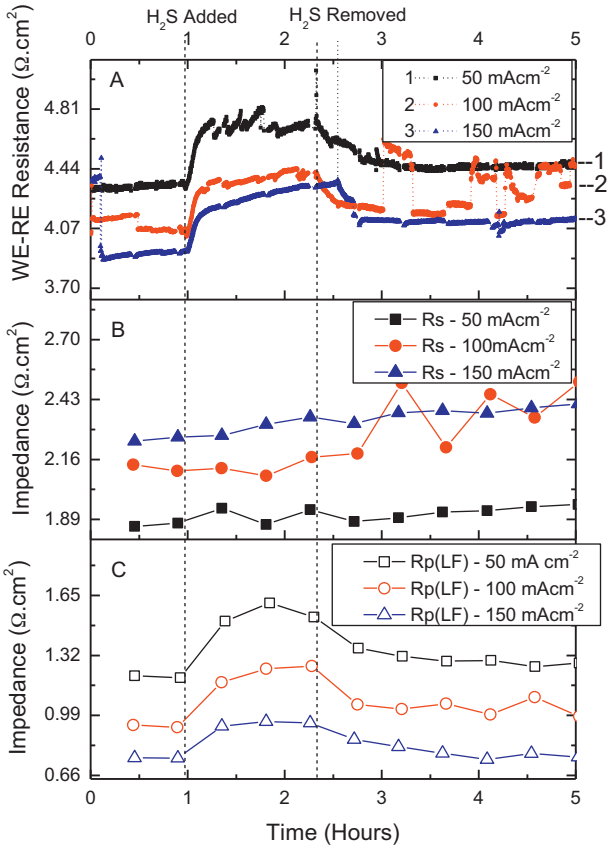

Fig. 3. (A) Uncompensated anode resistance measured by galvanostatic potentiometry; (B) and (C) equivalent circuit fitting results from impedance spectra, for exposure to 0.5 ppm H_2S and recovery in clean fuel at 715 °C at 0.05, 0.10, and 0.15 A cm^{-2}. Dotted lines indicate when H_2S was added to the gas stream and removed.

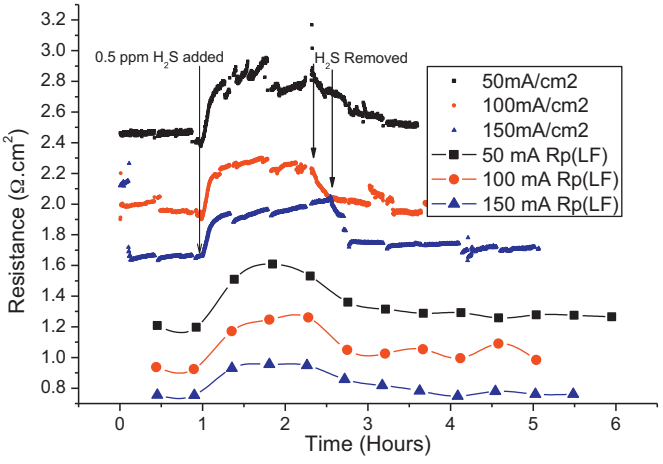

Fig. 4. Compensated anode resistance from potentiometry measurements calculated from the data in Fig. 3 (upper data sets), and polarization resistance from equivalent-circuit modelling of impedance measurements ($R_p(LF)$).

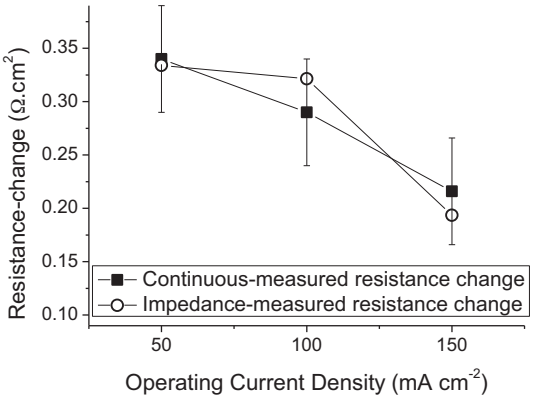

Fig. 5. Increase in anode resistance on adding 0.5 ppm H_2S as a function of current density, estimated from the data in Fig. 3. Error bars reflect the uncertainty due to the instability of the continuous measurement.

of O^{2-}, and hence a higher rate of desorption.

$$S_{(ads)} + 2O^{2-} \rightleftharpoons SO_2(g) + 4e^- \quad (1)$$

Future work will aim to discover if there is a limiting current density above which the anode polarization resistance does not increase with H_2S addition; this is likely to be closely linked to the activation energy for this electrochemical sulphur oxidation mechanism.

3.2. Effect of $p(H_2S)$ and temperature at constant current density

A second cell was reduced and characterized in the same way as the cell in Section 3.1, and exposed to concentrations of 0.5 ppm, 1 ppm and 3 ppm H_2S under a constant current load of 0.1 A cm^{-2} at 715 °C. The cell was then exposed to 1 ppm H_2S at 0.1 A cm^{-2} at temperatures of 700 °C, 730 °C, and 750 °C, with recovery in clean fuel after each poisoning. The i-V behaviour of the cell was measured between each poisoning and recovery to monitor any permanent degradation from each exposure. The impedance-corrected overpotential–current density curves are shown in Fig. 6. The anode resistance actually decreased from the initial measurement after the first sulphur poisoning experiment, after which the anode overpotential at 0.10 A cm^{-2} increased by ~0.5% between each successive poisoning and recovery experiment. It is assumed that this is due to underlying background degradation and that the cell recovers completely from the sulphur poisoning.

Fig. 7 shows the cell potential and equivalent circuit fitting results for the varied pH_2S experiment. The impedance spectra of this cell differed slightly from the previous cell in that the high-frequency (parallel R-CPE) component was almost entirely overlapped by the low-frequency arc, as shown in Fig. 2(C). Therefore, for simplicity, the spectra were fitted to an equivalent circuit with only one R-CPE parallel component (R_p) and one series resistance (R_s) (Fig. 2(D)).

The extracted data for the increase in anode polarization resistance (Fig. 7(C)) show the expected trend of initial rapid increase in resistance followed by a more-or-less stable value, which slowly recovers to the initial performance on switching back to clean fuel. Higher concentration of H_2S gives a slightly higher increase in R_p, similar to results previously reported elsewhere [3,9].

The most notable feature of the data presented in Fig. 7, however, is that as pH_2S is increased there is a secondary degradation occurring after the initial drop in cell performance. This secondary degradation affects the series component of the impedance, implying the formation of an insulating phase caused by the increased concentration of sulphur. This will be discussed further in subsequent paragraphs.

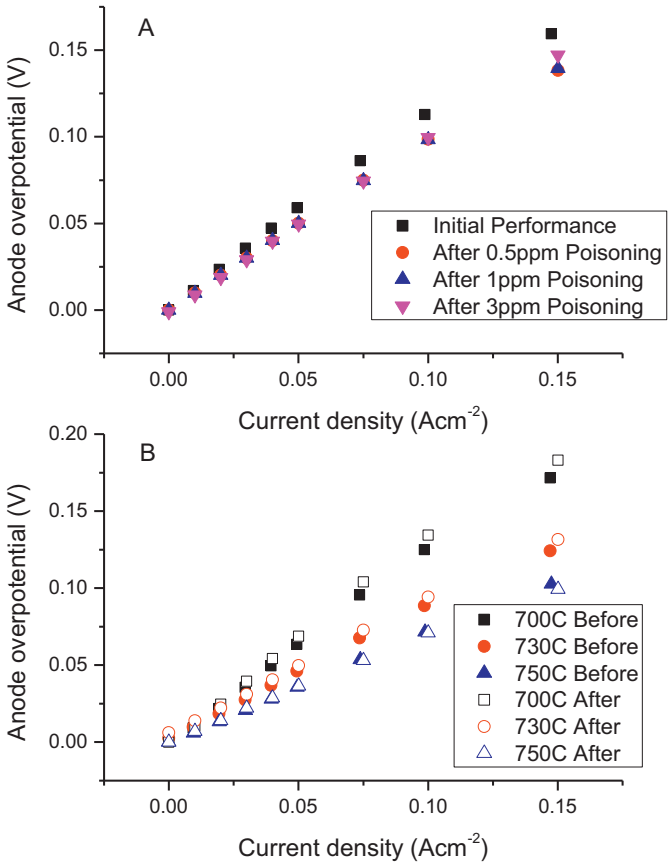

Fig. 6. Polarization performance of test cell for Section 3.2 before and after each successive poisoning experiment.

Fig. 8 shows the results for exposure to 1 ppm H_2S at 0.1 A cm^{-2} at three different temperatures. Looking initially at the trend for R_p in the lower panel, the initial stepwise decrease in performance follows the trend expected from the established literature on sulphur poisoning behaviour, i.e., a smaller increase in R_p occurs at higher temperatures. However, there is also a secondary degradation in the data at 750 °C, and to a much lesser extent at 730 °C, which again corresponds to an increasing ohmic resistance, similar to the trend in Fig. 7.

It is important to note that this dramatic increase in R_s is accompanied by a large degree of instability in the measurements as can be seen by the larger fitting errors on the impedance spectra, and the scatter in the measurements of the potentiometry data.

Indeed, for the data at 750 °C some of the impedance spectra were unusable. However, the stability returned after just 2–3 h from switching to clean fuel.

The experiment at 750 °C was repeated at a higher current density of 0.16 A cm^{-2}, in order to examine the performance at a similar anode overpotential to the lower temperature experiments. The data are shown together with the data for the 0.10 A cm^{-2} poisoning in Fig. 9, and show that the higher current density does mitigate the ohmic degradation, though not completely. The abrupt recovery at ~5 h occurred when the spring-loaded connection to the current collector was adjusted. This implies the degradation may be linked to the interface of the anode surface with the current collectors.

4. Discussion

Hansen [18] reported an empirically derived isotherm for calculating the sulphur coverage on Ni surfaces at given conditions. Using this, the theoretical surface coverage in the conditions used was

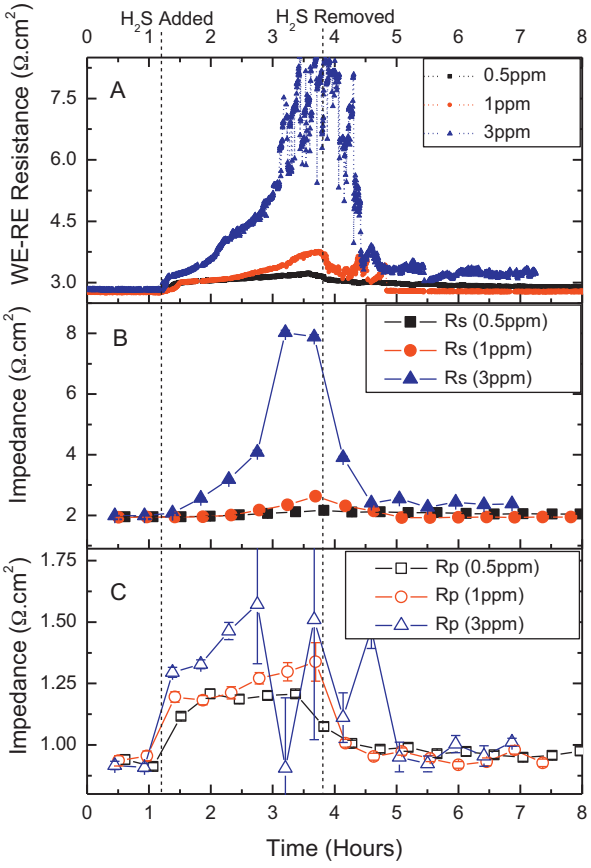

Fig. 7. (A) Uncompensated anode resistance from potentiometry at 0.10 A cm^{-2}, T = 715 °C; (B) and (C) modelling parameters from equivalent circuit fitting of periodic impedance spectra taken during the same 0.10 A cm^{-2} potentiometry. Dotted lines indicate when 0.5 ppm, 1 ppm and 3 ppm H_2S was added to the gas stream and removed.

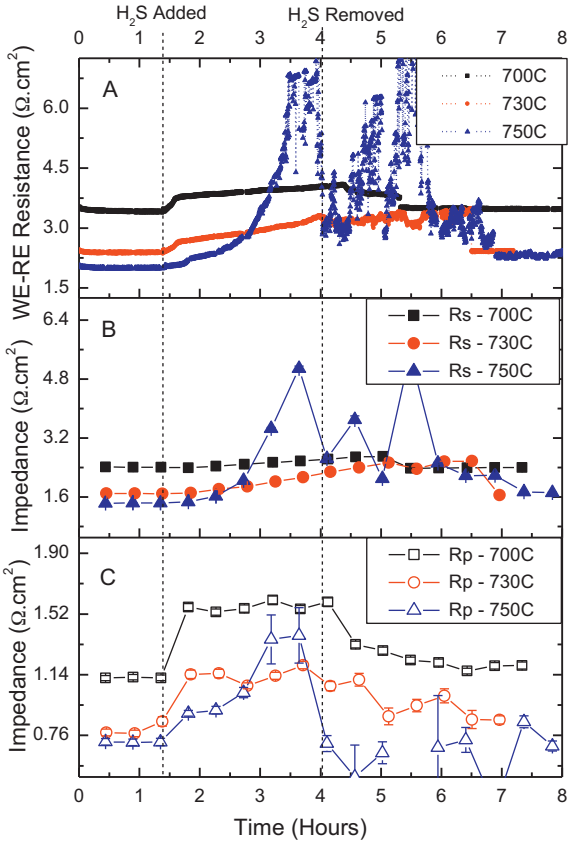

Fig. 8. (A) Uncompensated anode resistance from potentiometry at 0.10 A cm^{-2}, T = 700 °C, 730 °C and 750 °C; (B) and (C) modelling parameters from equivalent circuit fitting of periodic impedance spectra taken during the same 0.10 A cm^{-2} potentiometry. Dotted lines indicate when 1 ppm H_2S was added to the gas stream and removed.

calculated, as shown in Table 1. A higher sulphur coverage would account for the larger increase in R_p observed at lower temperature and/or higher pH_2S. However, higher sulphur coverage does not account for the ohmic degradation observed for 1 ppm H_2S at 750 °C, where the theoretical sulphur coverage is the same as for 0.5 ppm H_2S at 715 °C.

The authors have recently published microstructural investigations of identical cells to those used here, [14] which showed significant faceting, or step-formation, on the surface of the Ni grains. This may be related to dissolution of S in the Ni at the surface, which would account for the increase in series resistance observed. However, this electrochemical behaviour seen here has not previously been reported in any of the literature surveyed, which was predominantly on Ni–YSZ cermet anodes. The anodes used in this work were Ni–CGO cermets. This suggests it is not the Ni phase on its own which is contributing to the poisoning behaviour, but there may be a change in reactivity of Ni due to the electrolyte phase in the cermet.

Lohsoontorn et al. [11] observed similar electrochemical behaviour in Ni–CGO cermet anodes, which would suggest that a change is occurring in the CGO phase to affect the ohmic resistance of the anode. Lohsoontorn et al. also studied the thermodynamics of the bulk Ce–O–S system [13], which shows the operating

Table 1
Fractional coverage of S on Ni surface calculated using the isotherm in Ref. [18].

T/°C	T/K	θs			
		pH_2S	0.5 ppm	1 ppm	3 ppm
		pH_2S/pH_2	1.0×10^{-06}	2.0×10^{-06}	6.0×10^{-06}
700	973		0.80	0.82	0.87
715	988		0.79	0.82	0.86
730	1003		0.78	0.81	0.85
750	1023		0.76	0.79	0.84

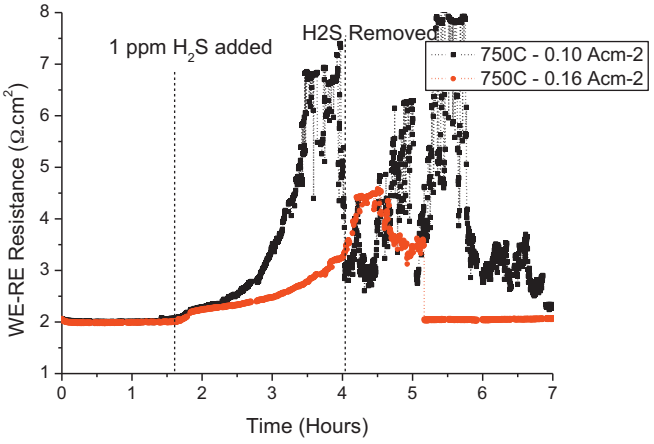

Fig. 9. Uncompensated anode resistance at 750 °C for 1 ppm H_2S exposure at fixed current. Squares (black online) – 0.10 A cm^{-2}, diamonds (red online) – 0.16 A cm^{-2}. (For interpretation of the references to color in this figure legend, the reader is referred to the web version of the article.)

conditions used here are close to the phase boundary between the reduced-state $CeO_{1.83}$ phase and Ce_2O_2S, though the effect of potential on the Ce–O–S phase behaviour has not yet been investigated. Further investigation is required to verify whether changes in the CGO account for the temperature and potential dependence of this phenomenon.

5. Conclusions

It has been shown that H_2S poisoning of Ni–CGO anodes with 0.5 ppm H_2S for around 90 min causes a rapid increase in anode polarization resistance that is fully recoverable in clean fuel. The degree of poisoning, measured by the increase in anode polarization resistance, was found to be lower for higher current density operation. This is thought to be a result of higher flux of O^{2-} from the electrolyte causing oxidative desorption of $S_{(ads)}$ to $SO_2(g)$ at triple-phase boundaries.

At higher H_2S concentrations (up to 3 ppm at 715 °C) and at higher temperatures (up to 750 °C) a secondary degradation was observed in addition to the primary rapid increase in R_p. This additional degradation was caused by an increase in series resistance, and it is suggested that this increase may be a result of near-surface microstructural changes in the Ni and/or CGO component of the cermet, possibly due to dissolution of S at the surface.

Further investigation using surface-analytical techniques is ongoing, as well as development of an *in situ* optical microscopy SOFC rig for investigation of the surface reactions occurring during electrochemical oxidation of adsorbed H_2S in H_2 using Raman spectroscopy.

Acknowledgements

This work was funded under the EPSRC Supergen Fuel Cells Consortium. One of the authors (E.B.) is supported by the Janet Watson Scholarship.

References

[1] C.H. Bartholomew, Applied Catalysis A – General 212 (2001) 17–60.
[2] C.H. Bartholomew, P.K. Agrawal, J.R. Katzer, Advances in Catalysis 31 (1982) 135–242.
[3] S. Zha, Z. Cheng, M. Liu, Journal of the Electrochemical Society 154 (2007) 201.
[4] P. Marecot, E. Paraiso, J.M. Dumas, J. Barbier, Science 80 (1992) 89–97.
[5] G.J. Offer, J. Mermelstein, E. Brightman, N.P. Brandon, Journal of the American Ceramic Society 92 (2009) 763–780.
[6] J.N. Kuhn, N. Lakshminarayanan, U.S. Ozkan, Journal of Molecular Catalysis 282 (2008) 9–21.
[7] Y. Matsuzaki, I. Yasuda, Solid State Ionics 132 (2000) 261–269.
[8] K Sasaki, K. Susuki, A. Iyoshi, M. Uchimura, N. Imamura, H. Kusaba, et al., Journal of the Electrochemical Society 153 (2006) 0.
[9] J.F. Rasmussen, A. Hagen, Journal of Power Sources 191 (2009) 534–541.
[10] K. Sasaki, K. Haga, J. Yamamoto, K. Dobuchi, in: European Solid Oxide Fuel Cell Forum, 2008, p. b1003.
[11] P. Lohsoontorn, D. Brett, N. Brandon, Journal of Power Sources 183 (2008) 232–239.
[12] Z. Cheng, S. Zha, M. Liu, Journal of Power Sources 172 (2007) 688–693.
[13] P. Lohsoontorn, D.J. Brett, N.P. Brandon, Journal of Power Sources 175 (2008) 60–67.
[14] D.G. Ivey, E. Brightman, N. Brandon, Journal of Power Sources 195 (2010) 10.
[15] D.J. Brett, A. Atkinson, N.P. Brandon, S.J. Skinner, Chemical Society Reviews 37 (2008) 1568–1578.
[16] G. Offer, P. Shearing, J. Golbert, D.J. Brett, A. Atkinson, N.P. Brandon, Electrochimica Acta 53 (2008) 7614–7621.
[17] P.V. Aravind, J.P. Ouweltjes, J. Schoonman, Journal of the Electrochemical Society 156 (2009) B1417.
[18] J.B. Hansen, Electrochemical and Solid-State Letters 11 (2008) B178.